Visualization of Global Trade-offs in Aerodynamic Problems by ARMOGAs

Daisuke Sasaki[1], and Shigeru Obayashi[2]

[1]School of Engineering, University of Southampton, Highfield, Southampton, SO17 3SP, United Kingdom
D.Sasaki@soton.ac.uk
[2]Institute of Fluid Science, Tohoku University, Katahira 2-1-1, Sendai 980-8577, Japan
obayashi@ieee.org

Abstract. Global tradeoffs for aerodynamic design of Supersonic Transport (SST) have been investigated by Multi-Objective Evolutionary Algorithms (MOEAs). The objectives are to reduce both drag and sonic boom to make next-generation SST more feasible. Adaptive Range Multi-Objective Genetic Algorithms (ARMOGAs) are utilised for the efficient search. The trade-offs are analysed by Self-Organising Map (SOM), which provides a topology preserving mapping from the high dimensional space to two dimensions. ARMOGAs and SOM can be good design tools to conduct aerodynamic design optimisations and analyse the results.

1 Introduction

Multi-Objective Evolutionary Algorithms (EAs) are becoming popular in many fields since they provide a unique opportunity to address global trade-offs between multiple objectives by sampling a number of Pareto solutions. Especially in the field of aeronautical engineering, a series of studies for aerodynamic design of supersonic wings have been performed by the present authors [1-3]. Throughout these researches, the following two problems have been revealed: Enormous computational time and difficulties in analysis of non-dominated solutions. As high-fidelity Computational Fluid Dynamics (CFD) computations, such as Euler or Navier-Stokes computations, require a large computational time, efficient optimisers based on EAs are highly desired for the general use. A data mining technique is also necessary because it is not easy to analyse the non-dominated solutions after the optimisation. For example, four design objectives were used and the resulting non-dominated front was obtained as a three-dimensional surface in the four-dimensional objective function space. Although 766 non-dominated solutions were obtained in total, only a few solutions were examined in detail [3]. That was a typical case that computer produces/accumulates too much data. To make a good use of the large data, a data mining technique was necessary.

Dagstuhl Seminar Proceedings 04461
Practical Approaches to Multi-Objective Optimization
http://drops.dagstuhl.de/opus/volltexte/2005/241

In this paper, the Adaptive Range Multi-Objective Genetic Algorithms (ARMOGAs, [4]) and the Self-Organising Map (SOM, [5]) are applied to the aerodynamic design problem of Supersonic Transport (SST). The next generation SST still has many technical obstacles to overcome. One of them is high aerodynamic efficiency for an economic flight, and another is low sonic boom for an environmental issue. These demands have a severe trade-off, because the reduction of sonic boom often leads to an increase in drag [6]. Several innovative designs have been proposed for low-boom, low-drag SST configuration. One idea is to equip a canard for SST wing-fuselage configuration to obtain more lift near the nose with a slender fuselage. This configuration may allow realisation of a low boom, while minimising drag. Two objectives of minimising both drag and boom will be optimised efficiently by ARMOGAs, which have been developed to reduce the number of evaluations. This would be an advantage for engineering design problems that require large computational time for each evaluation. After non-dominated solutions that form trade-offs are obtained, SOM is applied to the solutions. As the SOM is a cluster analysis tool for high-dimensional data, the trade-offs can be successfully visualized. By these results, the viability of the SST wing-fuselage configuration with a canard for low drag and boom will be discussed.

2 Adaptive Range Multi-Objective Genetic Algorithms

To reduce the large computational burden, the reduction of the total number of evaluations is needed. On the other hand, a large string length is necessary for real parameter problems. Adaptive Range Genetic Algorithms (ARGAs), originally proposed by Arakawa and Hagiwara, is a quite unique approach to solve such problems efficiently [7]. Oyama developed real-coded ARGAs and applied them to a transonic wing optimisation [8]. Both methods make use of range adaptation for effective search of the best solution for single-objective optimisation problems. In addition, archiving and constraint-handling techniques are considered to select better solutions to determine new search range.

The basis of the present ARMOGAs is the same as real-coded ARGAs, but a straightforward extension may cause a problem in the diversity of the population. Therefore, ARMOGAs have been developed based on ARGAs to deal with multiple Pareto solutions for multi-objective optimisation.

ARMOGAs have been developed to consider the following things: sophisticated encoding system for multiple solutions, archiving technique, and constraint-handling technique. The encoding system is based on the normal distribution with the plateau region as shown in Fig. 1. The selected superior designs are located in the plateau region, and the normal distribution region is determined based on the population statistics to preserve the diversity of candidate solutions. The solutions, which have higher fitness values based on Pareto ranking method for all solutions obtained so far, are selected to determine the search range for unconstrained problems. For constrained problems, constrained Pareto ranking method is used to evaluate all solutions. In addition to

the constrained Pareto ranking method, infeasible solutions that violate the constraint slightly are selected to search near the boundary between feasible and infeasible solutions.

A flowchart of ARMOGAs is shown in Fig. 2. The range adaptation is carried out every *M* generations. The new decision space is determined based on the statistics of selected better solutions. The new population is then randomly generated in the new decision space. This helps to maintain the diversity of solutions. Subsequently, all the genetic operators are applied to the new design space.

In the present ARMOGAs, the fitness value of each solution is determined by Fleming and Fonseca's Pareto-ranking method [9] coupled with fitness sharing approach [10]. Each individual is assigned a rank according to the number of individuals dominating it. The assigned fitness values are divided by the niche count, which is calculated by summing the sharing function values. Each new parent set is selected from the present population and the previous parent set by CHC [11] and Stochastic Universal Selection (SUS, [12]) according to shared fitness values. SBX [10] and polynomial mutation [10] methods are adopted for crossover and mutation.

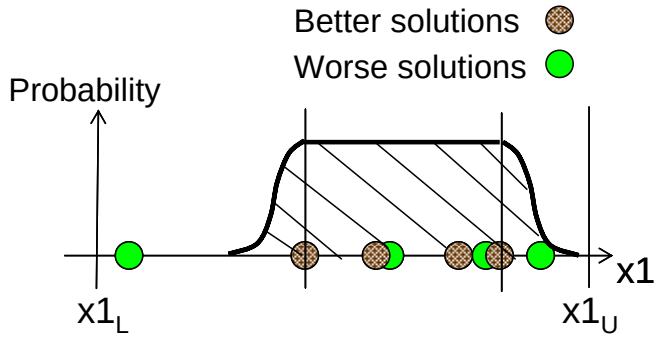

Fig. 1. Sketch of range adaptation

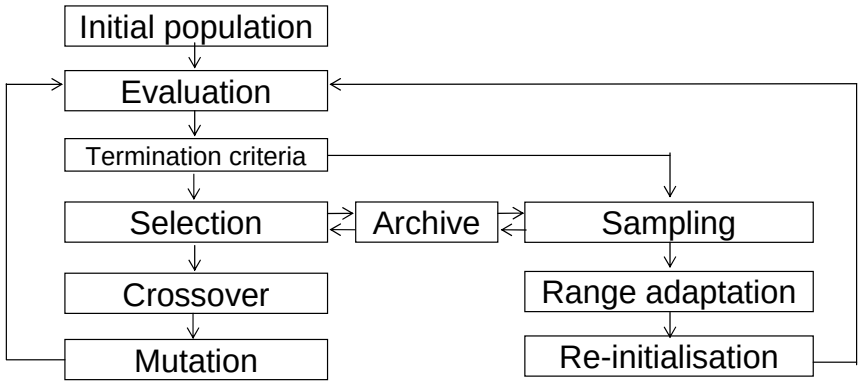

Fig. 2. Flowchart of ARMOGAs

3 Aerodynamic Optimisation by ARMOGAs

The objectives of the present aerodynamic optimisation are to reduce both drag and boom for canard-wing-fuselage configuration. The aerodynamic evaluation proceeds in the following order: geometry definition, unstructured mesh generation, and aerodynamic evaluation by Euler computation. In this study, TAS-Code (Tohoku University Aerodynamic Simulation Code [13-18] is used for the mesh generation and the aerodynamic evaluation.

Design variables that determine the shape of wing-fuselage configurations equipped with a canard are composed of four groups: wing shape, canard shape, fuselage configuration, and wing lofting. Design variables for the wing shape was categorised to planform, warp shape and thickness distribution. Figure 3 shows the definition of the planform shape based on six design variables.

The planform shape of canard is defined as similar to the inboard of the main wing. The symmetric wing is assumed for the canard, and it is composed of planform shape and thickness distribution. In the system, thickness distribution is defined by Bézier surface having four control points at root and tip location, respectively.

Fuselage configuration was defined by the area-rule theory. The area-ruled fuselage is determined by the distribution of the cross-sectional area of the wing and the canard to satisfy the Sears-Haack Body.

Other design variables are used for wing lofting that indicates how to combine wing and fuselage, and canard and fuselage. The total number of design variables is 94.

In the present optimisation, one of the objective functions is to minimise drag coefficient (C_D) at a Mach number of 1.6 with fixed lift coefficient (C_L) of 0.125.

$$\text{Minimise } f_1 = C_D, \tag{1}$$

$$\text{subject to } 0.97\times C_{L,target} \le C_{L,design} \le 1.03 \times C_{L,target},\ C_{L,target}=0.125. \tag{2}$$

Second objective function is to minimize the difference between target and designed equivalent area distribution ($Ae(t)$) which is a summation of contribution from lift $A(t)$ and volume $B(t)$.

$$\text{Minimise } f_2 = \int_0^{l^*} \left| Ae_{design}(t) - Ae_{tar\cdot get}(t) \right| dt, \tag{3}$$

where l^* is set to the rear part position of the main wing.

In linear theory, low sonic boom flight can be achieved by realising Darden's equivalent area distribution [19]. Darden's and sample equivalent area distribution are plotted in Fig. 4.

In total, six constraints are imposed in the optimisation system. In addition to the wing volume, fuselage volume, and minimum fuselage diameter, the feasibility of the design is also considered. Table 1 shows the minimum constraint values of wing volume, fuselage volume and minimum fuselage diameter.

ARMOGAs were adopted as optimisers to reduce the number of CFD evaluations. In addition, Master-Slave type parallelisation was performed to reduce the computational time. Master processor manages ARMOGAs and slave processors conduct separate CFD computations for different individuals. After the range adaptation starts at the fifth generation, new ranges of design variables according to better solutions are determined every five generations. At the production of new individuals, such as by crossover, mutation, or re-initialisation, new individuals are generated repeatedly until they satisfy the constraints related to the geometry. The following settings were used.

- Number of individuals per generation: 8
- Number of generations: 50

Figure 5 shows the history of design improvements from the beginning to the final generations. Many initial SST configurations generated randomly were quite different from the modern aeroplane configuration. With increasing number of generations, more sophisticated geometries were generated. Finally, eight non-dominated solutions were obtained.

The low-boom design is selected to discuss the viability of canard-wing-fuselage configuration. The shape with pressure contours is shown in Fig. 6. Figure 7 shows the equivalent area distributions of designed configuration and Darden's. In this design problem, as the shape near the nose of the fuselage was determined by the area rule, both the equivalent area distributions near the nose were not similar. However, in other regions, both distributions were quite similar because of the canard, and the large swept back wing to obtain a great deal of lift at the rear of the fuselage.

Table 1. Geometrical constraints

Constraint	MinimumValue
Wing Volume	16,000 ft^3
Fuselage Volume	30,000 ft^3
Minimum Fuselage Diameter	11.68 ft

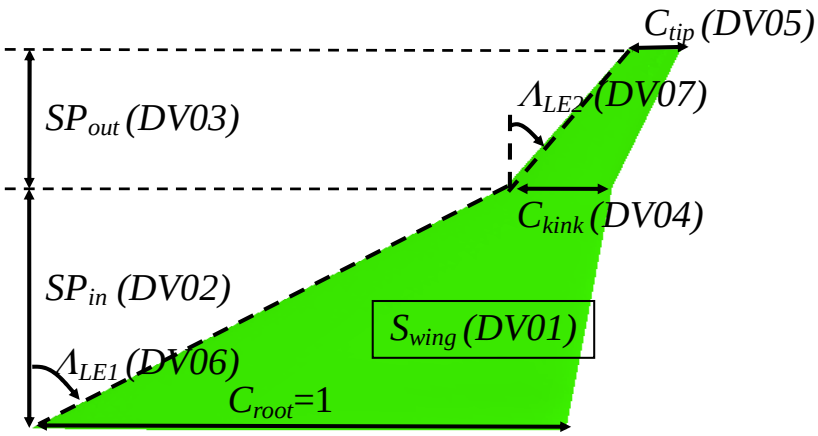

Fig. 3. Wing planform definition

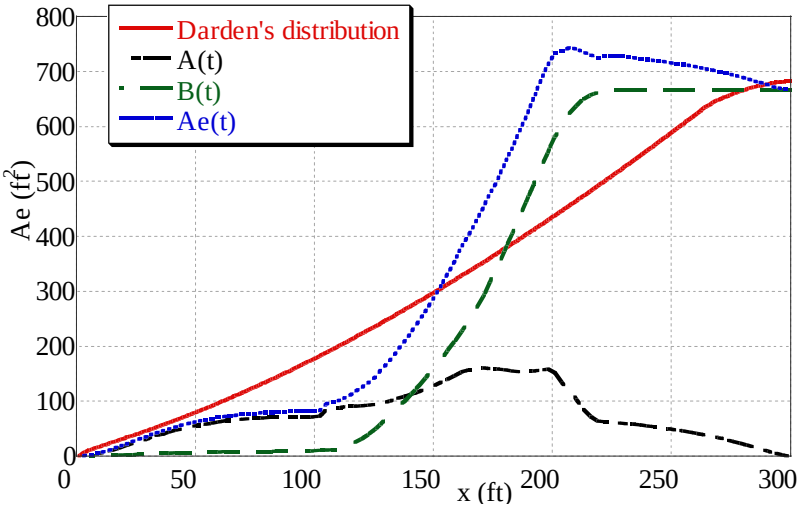

Fig. 4. Equivalent area distribution of Darden's and sample geometry

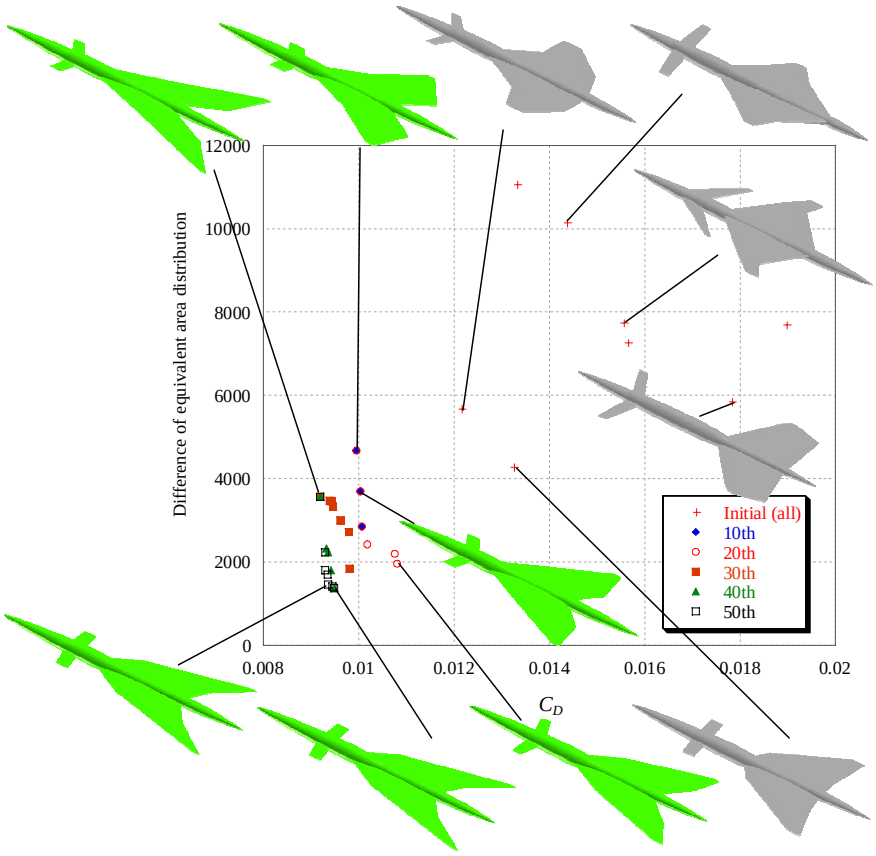

Fig. 5. Initial candidates and non-dominated solutions at 10th, 20th, 30th, 40th, 50th generations

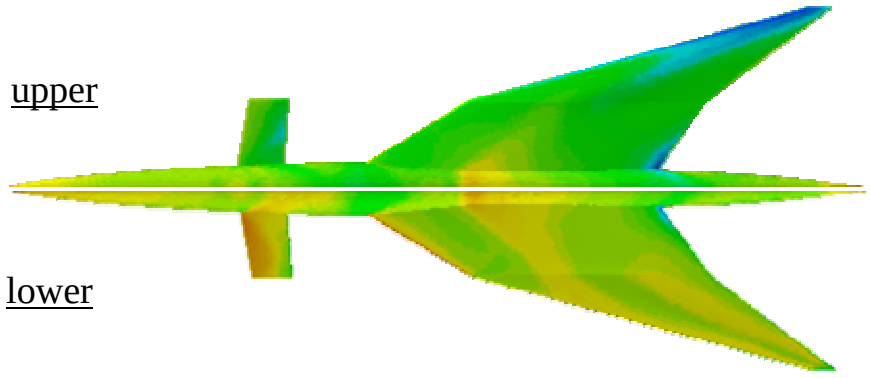

Fig. 6. Configuration of low-boom design with pressure contours on surface

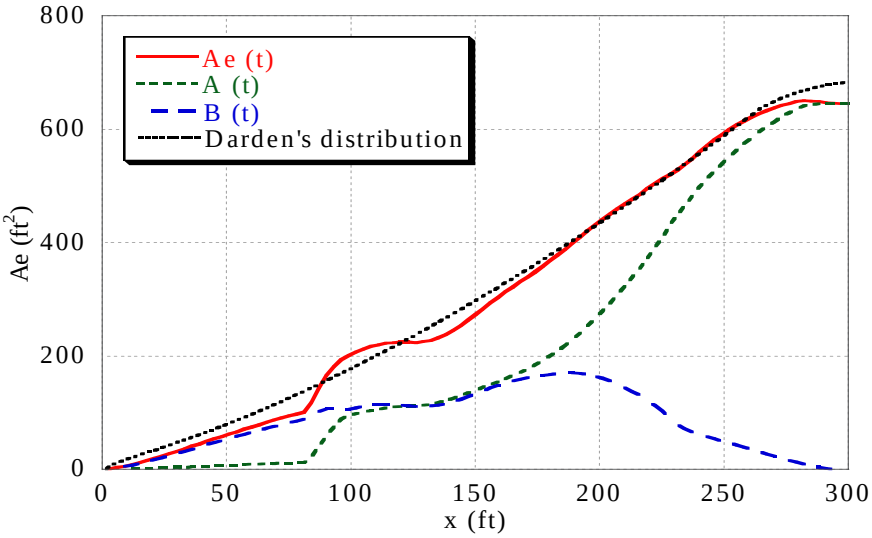

Fig. 7. Equivalent area distributions of the low-boom design and Darden

4 Self-Organising Map

Self-Organising Map is a two-dimensional array of neurons: $\mathbf{M} = \{\mathbf{m}_1 \cdots \mathbf{m}_{p\times q}\}$. One neuron is a vector called the codebook vector $\mathbf{m}_i = \lfloor m_{i_1} \ \cdots \ m_{i_n} \rfloor$. This has the same dimension as the input vectors. The neurons are connected to adjacent neurons by a neighborhood relation. This dictates the topology, or the structure, of the map. Usually, the neurons are connected to each other via rectangular or hexagonal topology as shown in Fig. 8. One can also define a distance between the map units according to their topology relations. Immediate neighbors (the neurons that are adjacent) belong to the neighborhood *Nc* of the neuron m_c. The neighborhood function should be a decreasing function of time: *Nc=Nc(t).*

The training consists of drawing sample vectors from the input data set and "teaching'" them to the SOM. The teaching consists of choosing a winner unit by means of a similarity measure and updating the values of codebook vectors in the neighborhood of the winner unit. This process is repeated a number of times. In one training step, one sample vector is drawn randomly from the input data set. This vector is fed to all units in the network and a similarity measure is calculated between the input data sample and all the codebook vectors. The best-matching unit is chosen to be the codebook vector with greatest similarity with the input sample. The similarity is usually defined by means of a distance measure. For example in the case of Euclidean distance the best-matching unit is the closest neuron to the sample in the input space.

The best-matching unit, usually denoted as $\mathbf{m}_c$, is the codebook vector that matches a given input vector x best. It is defined formally as the neuron for which $\|\mathbf{x} - \mathbf{m}_c\| = \min_i \{\|\mathbf{x} - \mathbf{m}_i\|\}$. After finding the best-matching unit, units in the SOM are updated. During the update procedure, the best-matching unit is updated to be a little closer to the sample vector in the input space. The topological neighbors of the best-matching unit are also similarly updated. This update procedure stretches the best-matching unit and its topological neighbors towards the sample vector. The update procedure is illustrated in Fig. 9. The codebook vectors are situated in the crossings of the solid lines. The topological relationships of the SOM are drawn with lines. The input fed to the network is marked by x in the input space. The best-matching unit, or the winner neuron is the codebook vector closest to the sample, in this example the codebook vector in the middle above **x**. The winner neuron and its topological neighbors are updated by moving them a little towards the input sample. The neighborhood in this case consists of the eight neighboring units in the figure. The updated network is shown in the same figure with dashed lines. In the following, SOMs were generated in the hexagonal topology by using Viscovery® SOMine Plus 4.0 (http://www.eudaptics.com/technology/somine.html).

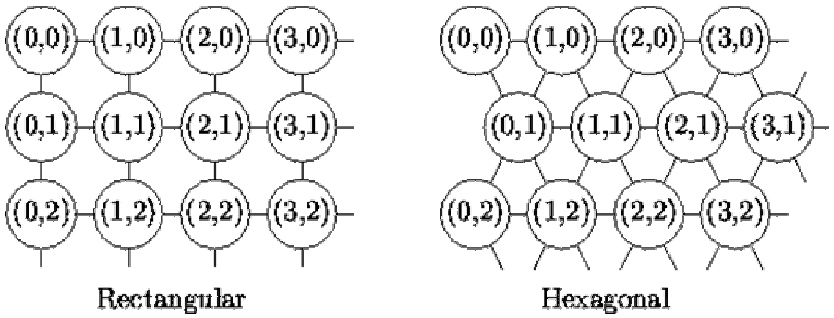

Fig. 8. Different topologies used in SOM

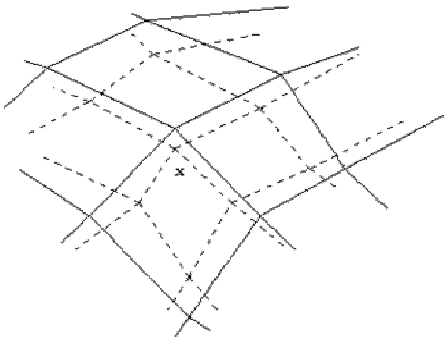

Fig. 9. Updating the best matching unit and its neighbour

5 Visualisation by SOM

All seven non-dominated solutions obtained during the present optimisation were mapped onto SOM according to the scaled objective function values. The resulting SOM is shown in Fig. 10. The map consists of three clusters based on the similarity of seven non-dominated solutions' in terms of the objective-function values. Three non-dominated solutions (S1, S2, S3) that represent respective cluster are also drawn in the figure. The corresponding objective-function values (OBJ1: drag, OBJ2: boom) are then plotted in Fig. 11 where white indicates low value, and dark colour indicates high value. The lower left cluster contains the extreme approximate Pareto solution of the minimum drag. The upper left cluster contains the extreme approximate Pareto solution of the minimum boom. The other cluster has medium values of drag and boom. As seven non-dominated solutions can be divided into three groups, three configurations that represent each cluster would be enough to understand the trade-offs involved in this optimisation problem. Table 2 shows the aerodynamic performance and geometrical values of the three solutions. High lift to drag ratio (*L/D*) indicates the high aerodynamic performance in the table. Three shapes achieve different values of *L/D* and boom, however, fuselage volumes and minimum fuselage diameters of the three configurations are almost the same. This indicates the canard configuration has an effect to obtain the lift at the fore part while maintaining the size of the fuselage.

To understand the trade-off among design variables, the 94 design variables of seven non-dominated solutions were mapped onto SOM as shown in Fig. 12. Different from the cluster from seven non-dominated solutions in Fig. 10, 94 design variables are categorized based on their similarity. Design variables are categorized into 13 clusters. Figure 13 shows the same SOM coloured by three solutions (S1, S2, S3). Some clusters, for example, (C1, C2) show large difference of values among three designs, other clusters, for example, (C3, C4) show little difference. Four design variables (DV27, DV86, DV02, DV05) are selected from the above four clusters C1, C2, C3, C4, respectively, for comparison purposes. Figure 14 shows the four design-variable values of seven non-dominated solutions for objective functions. As DV02 (inboard span length) and DV05 (chord length at tip) are constant for both objective functions, these two design variables can be fixed for the further optimisation. However, DV27 (one of the design variables related to the height of camber) has an effect on the boom strength. In addition, larger value of DV86 (one of the design variables related to the height of thickness for canard) tends to increase the drag while decreasing the boom. These analyses would be useful to determine the influence of the design variables on the objective functions.

Table 2. Typical design specifications of three non-dominated solutions

	S1	S2	S3
L/D	13.64	13.20	13.39
Difference of Ae (t)	3555	1369	1449
Fuselage volume (ft^3)	32834	32933	32610
Minimum fuselage diameter (ft)	11.80	11.79	11.84
Wing total volume (ft^3)	16225	16365	16192

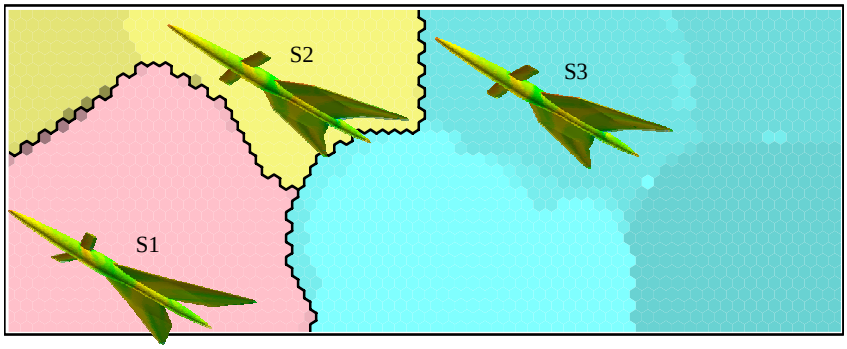

Fig. 10. SOM of objective function space with shapes of three non-dominated solutions

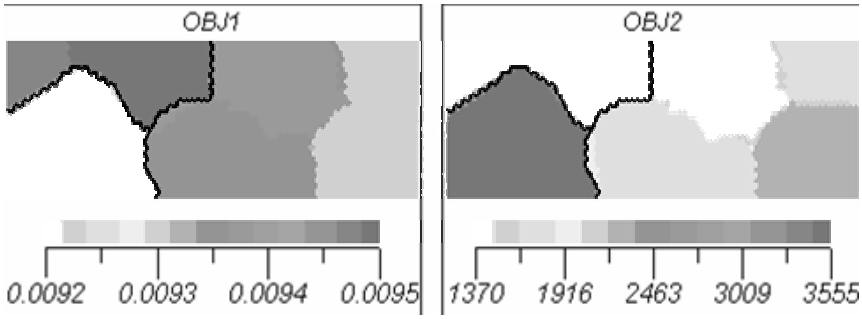

Fig. 11. SOM of objective function space coloured by each objective function

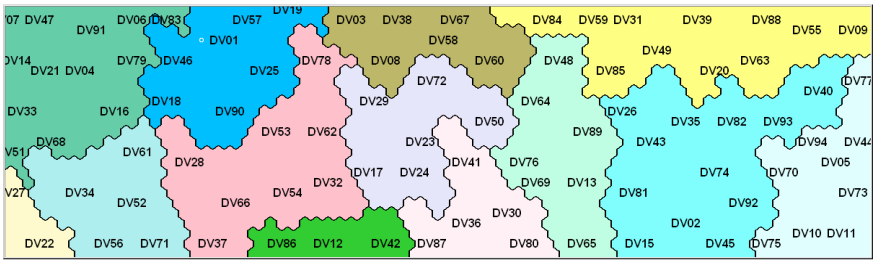

Fig. 12. SOM of design variable space

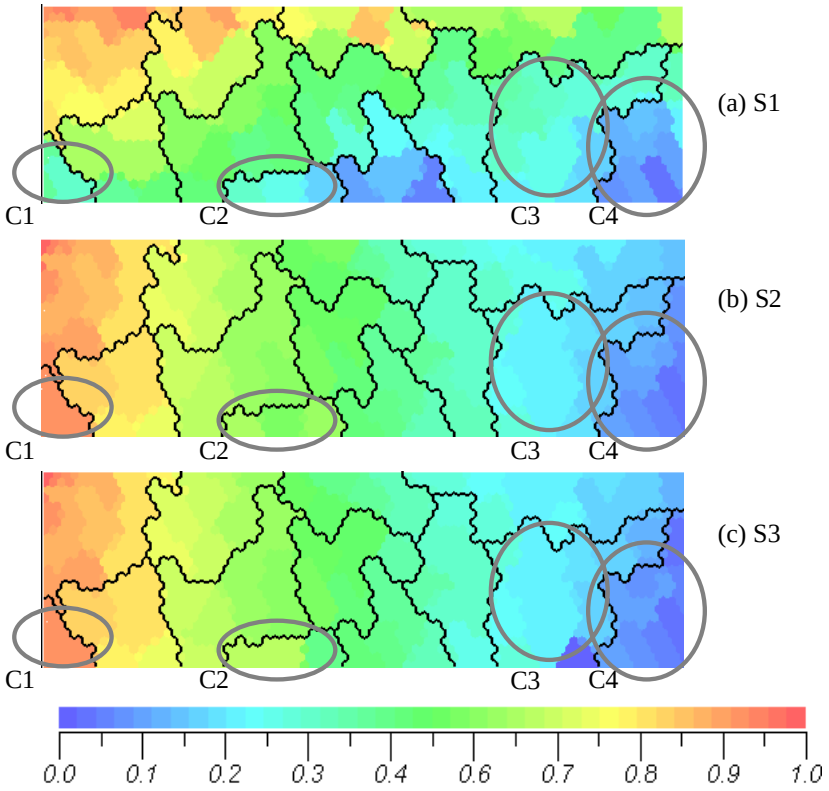

Fig. 13. Design variable space coloured by three non-dominated solutions

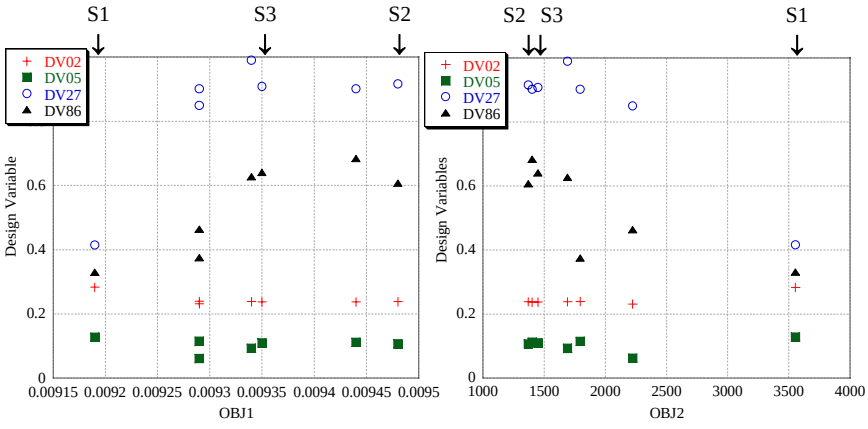

(a) C_D (b) Difference of Equivalent Area Distribution

Fig. 14. Four design variable distributions of seven non-dominated solutions

6 Conclusion

In this study, real-coded ARMOGAs, the aim of which was to find non-dominated solutions efficiently, has been applied to the aerodynamic optimisation problem of SST. Because of the system utilising both ARMOGAs and Master-Slave type parallelisation for each Euler computation, seven non-dominated solutions could be obtained efficiently. The equivalent area distributions of the low-boom design were quite similar to Darden's low-boom distribution by means of the canard and the swept back wing.

Self-Organising Map has also been applied to analyse seven non-dominated solutions. All solutions are mapped onto the SOM according to objective function values, and seven non-dominated solutions were divided into three clusters. By analysing the influence of design variables on objective function values, the objectives are sensible only to some of the design variables. ARMOGA and SOM would be useful tools for optimisation and analysis.

References

1. Obayashi, S., Sasaki, D., Takeguchi, Y., Hirose, N.: Multiobjective Evolutionary Computation for Supersonic Wing-Shape Optimization. IEEE Trans. on Evolutionary Computation 4 2 (2000) 182-187
2. Sasaki, D., Obayashi, S., Sawada, K., Himeno, R.: Multiobjective Aerodynamic Optimization of Supersonic Wings Using Navier-Stokes Equations. CD-ROM Proc. ECCOMAS 2000 (2000)
3. Sasaki, D., Obayashi, S., Nakahashi, K.: Navier-Stokes Optimization of Supersonic Wings with Four Objectives Using Evolutionary Algorithm. J. Aircraft 39 4 (2002) 621-629
4. Obayashi, S., Sasaki, D., Oyama, A.: Finding Tradeoffs by using Multiobjective Optimization Algorithms. Trans. of Japan Society for Aeronautics and Space Sciences 47 155 (2004) 51-58
5. Kohonen, T.: Self-Organizing Maps. Springer, Berlin (1995)
6. Sasaki, D., Yang, G., Obayashi, S.: Automated Aerodynamic Optimization System for SST Wing-Body Configuration. Trans. of Japan Society for Aeronautics and Space Sciences 46 154 (2004) 230-237
7. Arakawa, M., Hagiwara, I.: Development of Adaptive Real Range (ARRange) Genetic Algorithms. JSME Int. J. C 41 4 (1998) 969-977
8. Oyama, A., Obayashi, S., Nakamura, T.: Real-Coded Adaptive Range Genetic Algorithm Applied to Transonic Wing Optimization. Applied Soft Computing 1 3 (2001) 179-187
9. Fonseca, C. M., Fleming, P. J.: Genetic Algorithms for Multiobjective Optimization: Formulation, Discussion and Generalization. Proc. Fifth Int. Conf. on Genetic Algorithms (1993) 416-423
10. Deb, K.: Multi-Objective Optimization using Evolutionary Algorithms. John Wiley & Sons, Ltd., Chichester (2001)
11. Eshelman, L.: The CHC Adaptive Search Algorithm: How to Have Safe Search When Engaging in Nontraditional Genetic Recombination. Foundations of Genetic Algorithms (1991) 265-283

12. Baker, J. E.: Reducing Bias and Inefficiency in the Selection Algorithm. Proc. Second Int. Conf. on Genetic Algorithms (1987) 14-21
13. Ito, Y., Nakahashi, K.: Direct Surface Triangulation Using Stereolithography Data, AIAA J. 40 3 (2002) 490-496
14. Ito, Y., Nakahashi, K.: Surface Triangulation for Polygonal Models Based on CAD Data. Int. J. for Numerical Methods in Fluids 39 1 (2002) 75-96
15. Sharov, D., Nakahashi, K.: A Boundary Recovery Algorithm for Delaunay Tetrahedral Meshing. Proc. 5th Int. Conf. on Numerical Grid Generation in Computational Field Simulations (1996) 229-238.
16. Sharov, D., Nakahashi, K.: Reordering of Hybrid Unstructured Grids for Lower-Upper Symmetric Gauss-Seidel Computations. AIAA J. 36 3 (1998) 484-486
17. Obayashi, S., Guruswamy, G. P.: Convergence Acceleration of an Aeroelastic Navier-Stokes Solver. AIAA J. 33 6 (1994) 1134-1141
18. Venkatakrishnan, V.: On the Accuracy of Limiters and Convergence to Steady State Solutions. AIAA Paper 93-0880 (1993)
19. Darden, C. M.: Sonic Boom Theory: Its Status in Prediction and Minimization. J. Aircraft 14 6 (1977) 569-576